

Supporting Information

Controlling the 3-D morphology of Ni–Fe-based nanocatalysts for the oxygen evolution reaction

Ryan Manso,^{1,†} Prashant Acharya,^{2,†} Shiqing Deng,^{3,4†} Cameron C. Crane;¹ Benjamin Reinhart,⁵
Sungsik Lee,⁵ Xiao Tong,⁶ Dmytro Nykypanchuk,⁶ Jing Zhu,⁴ Yimei Zhu,³ Lauren F.
Greenlee,^{2,*} and Jingyi Chen^{1,*}

¹Department of Chemistry and Biochemistry, University of Arkansas, Fayetteville, AR 72701,
USA

²Ralph E. Martin Department of Chemical Engineering, University of Arkansas, Fayetteville, AR
72701, USA

³Condensed Matter Physics and Materials Science Department, Brookhaven National
Laboratory, Upton, NY 11973, USA

⁴School of Materials Science and Engineering, Tsinghua University, Beijing 100084, P. R. China

⁵Advanced Photon Source, Argonne National Laboratory, Lemont, IL 60439, USA

⁶Center for Functional Nanomaterials, Brookhaven National Laboratory, Upton, NY 11973, USA

[†]These authors contributed to this work equally.

*Corresponding authors: chenj@uark.edu (synthesis, characterization) and greenlee@uark.edu
(electrocatalysis, characterization)

Reaction Yield and Cost Estimations. We used our best performing catalyst as an example to calculate the yield of synthesis and estimate the cost of the small scale synthesis. The synthesis involves 3 steps: step 1 - synthesis of NiO_x cores; step 2 - shelling with FeO_x; and step 3 - ligand exchange from oleylamine to PEG-COOH. The amount of Ni for each step was quantitatively measured by ICP-MS and used to calculate the reaction yield. The yield of each step was calculated using the actual measured value divided by the theoretical value from the reaction and reported as percentage yield. For step 1, the yield is >95% after purification. The high yield of NiO_x is the result of two factors: 1) the reaction is performed under relatively-high temperature that can drive the reaction nearly completion; and 2) the nanoparticle self-assembly effect due to their hydrophobic ligands is quite effective to collect all the nanoparticles during centrifugation purification. The yield for the shelling is ~90%, but the overall yield is ~60%. The major cause of the loss in the overall yield comes from the relatively-low recovery from the centrifugation after the particle surface is covered with water soluble ligands. This loss can be minimized by using filter centrifuge tubes with a molecular cutoff slightly larger than the molar mass of the ligands (e.g. 10,000 Da) or a combination of dialysis and lyophilization to remove excess ligands and then water.

The cost estimation of the small scale synthesis is listed below in **Table S1** for the three-step synthesis. Each synthesis yields ~7 mg catalysts for the cost of ~\$2.76, roughly ~\$0.4/mg. Similar small-scale synthesis for 10 mg Ir by simply reacting IrCl₃ (\$261.00/1g, Alfa Aesar) with NaBH₄ will cost about the same \$0.4/mg if assuming 100% yield. However, our 3-step synthesis has room to bring down the cost by optimizing the process. For example, we can eliminate the purification procedure before Fe shelling step because step 1 nearly 100% converts the Ni precursor to NiO_x. As the 3-step process becomes 2 step, the yield of the reaction can be improved by at least 10%.

We can further improve the yield of purification process mentioned above. It is expected that we can improve the overall yield of the reaction to ~90% that will bring down the cost to ~0.3/mg. The price can be further reduced by using less solvent due to reduction of reaction steps and using a cheaper ligand (i.e. poly(acrylic acid), \$45.80/5 g) or potentially replacing the ligand exchange process by other methods. Therefore, we estimate that the cost of small scale process can be reduced to 1/3 or 1/4 of the original price at ~\$0.1/mg. In the case of noble metal, there is not much room to lower the production cost because the overall price is limited by the source of noble metal precursors. Thus, we consider the catalysts are low-cost and viable for future development. As for scale up production, similar to all other chemical synthesis, the solution-based synthesis of our catalysts at a large scale or gram scale is feasible by either scaling up the batch synthesis or using flow chemistry. When the production is scaled up, the price will be significantly reduced as it can be seen in the industries from chemical to pharmaceutical productions.

Table S1. The estimated cost per small scale 3-step synthesis for NiO_x-NiO_x/FeO_x core-shell nanocatalysts

Chemicals	Price	Amount used/synthesis	Price/synthesis
Ni(acac) ₂	\$39.70/25 g (Alfa Aesar)	51.5 mg	\$0.08
Octadecene	\$33.03/1 L (Acros)	9 mL	\$0.30
Oleylamine	\$132.00/500 g (Sigma-Aldrich)	1.2 mL	\$0.32
Trioctylphosphine	\$42.71/100 mL (Alfa Aesar)	1 mL	\$0.43
Fe(CO) ₅	\$35.10/25 g (Alfa Aesar)	20 uL	\$0.03
PEG-COOH	\$800.00/10 g (JenKem)	10 mg	\$0.80
Toluene*	\$120/19 L (VWR)	10 mL	\$0.06
Ethanol*	\$23.85/3.8 L (KOPTEC)	50 mL	\$0.31
Chloroform*	\$21.42/1 L (VWR)	10 mL	\$0.21
Hexane*	\$94.79/19 L (VWR)	45 mL	\$0.22
Total			\$2.76

Elemental Quantifications using Electron Microscopy.¹ Elemental quantifications were performed on the 2D maps of Fe L_{2,3} edge and Ni L_{2,3} edge using EELS QUANTIFICATION plug-in in Digital Micrograph commercial software. The quantitative analysis is based on the

fundamental relationship, given by $I_k = NI_0\sigma_k$, where I_0 represents the unscattered (zero-loss) intensity and N is the areal concentration (atoms /nm²) of the element contributing to the ionization edge k , I_k is the sum of all counts in that edge, and σ_k is the cross-section for ionization. Considering that a certain fraction of the electrons is intercepted by the angle-limiting aperture, partial cross-section $\sigma_k(\beta, \Delta)$ for energy losses within a range of the ionization threshold and for scattering angles up to β the above relationship should be used in the above relationship. β and Δ represent the scattering capture semi-angle angle (10.42 mrad) and signal integration width, respectively. After removing plural scattering from spectra *via* Fourier-Log deconvolution, atomic ratios of two elements (Ni and Fe) can be determined by

$$R_{Ni/Fe} = \frac{N_{Ni}}{N_{Fe}} = \frac{I_{LNi}^1(\beta, \Delta_{Ni}) \sigma_{LFe}(\beta, \Delta_{Fe}) F_{1Fe}}{I_{LFe}^1(\beta, \Delta_{Fe}) \sigma_{LNi}(\beta, \Delta_{Ni}) F_{1Ni}},$$

where $\Delta_{Fe} = \Delta_{Ni} = 40$ eV, $\sigma_{LNi}(\beta, \Delta)$ and $\sigma_{LFe}(\beta, \Delta)$ are partial cross-sections of Ni and Fe, respectively. In this algorithm, partial cross-sections are determined by calculating the energy-differential cross-section, $d\sigma/dE$, for the L-edge and integrates it over the specified signal integration energy-range. Hartree-Slater model was used for calculations. Based on our setups, $\sigma_{LNi}(\beta, \Delta)$ and $\sigma_{LFe}(\beta, \Delta)$ were determined as 310 ± 31 barns and 194 ± 19 barns (A barn is 10^{-28} m²), respectively. F_{1Fe}/F_{1Ni} is used to correct the incident beam convergence, which was computed at each $d\sigma/dE$.

Calculation of turn over frequency (TOF). The TOF was calculated based on the protocol established in the work of Stevens *et.al.*² TOF is defined in eq. 1.

$$\text{TOF} = \frac{\frac{\text{current}}{4F}}{\text{mol active sites}} \quad (1)$$

where F is Faraday's constant. The value for current was read at an overpotential of 400 mV and Ni atoms is considered as the active sites. The amount of Ni active sites on the electrode surface was estimated based on either ICP-MS analysis ($\text{TOF}_{\text{ICP-MS}}$) or redox wave ($\text{TOF}_{\text{redox wave}}$). For the former, the number of Ni active sites in moles is the amount of Ni placed on the electrode based on data obtained from ICP-MS. For the latter, the number of Ni active sites N is based on the amount of charge Q in coulombs (C) involved in the anodic wave using eq. 2.

$$N = \frac{Q}{mF} \quad (2)$$

where m is number of electrons transferred for the anodic reaction of Ni and F is Faraday's constant. Based on literature, $\text{TOF}_{\text{redox wave}}$ were calculated based on the assumption of either $1e^-$ transfer or $1.5e^-$ transfer, thereby m being either 1 or 1.5 in our calculation.^{2,3} The charge Q involved in the anodic reaction of Ni can be calculated using eq. 3.

$$Q = \frac{1}{\nu} \int IdE \quad (3)$$

where ν is the scan rate in V/s, I is current in amperes (A), and E is potential in volts (V). The value for $\int IdE$ was obtained by integrating anodic peak of Ni in the CV curve of the corresponding catalyst. The integration was not compensated with uncompensated resistance during data collection such that the current magnitude has no dependence on the sweep rate.

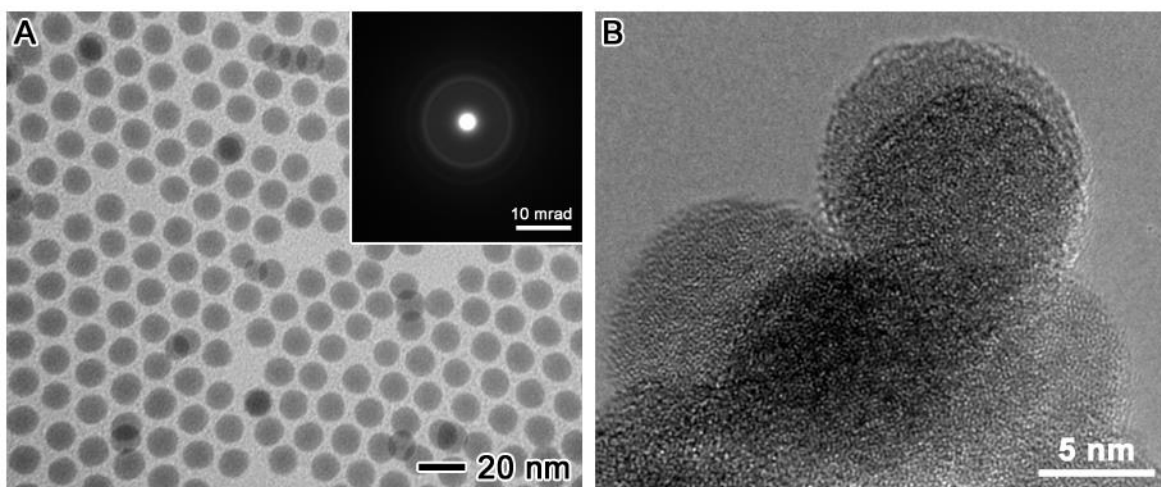


Figure S1. TEM characterization of NiO_x nanoparticles: (A) TEM image overview with the inset of electron diffraction pattern; and (B) HRTEM image. These NiO_x nanoparticles are spherical shape with an average size of 12.4 nm and have poor crystallinity.

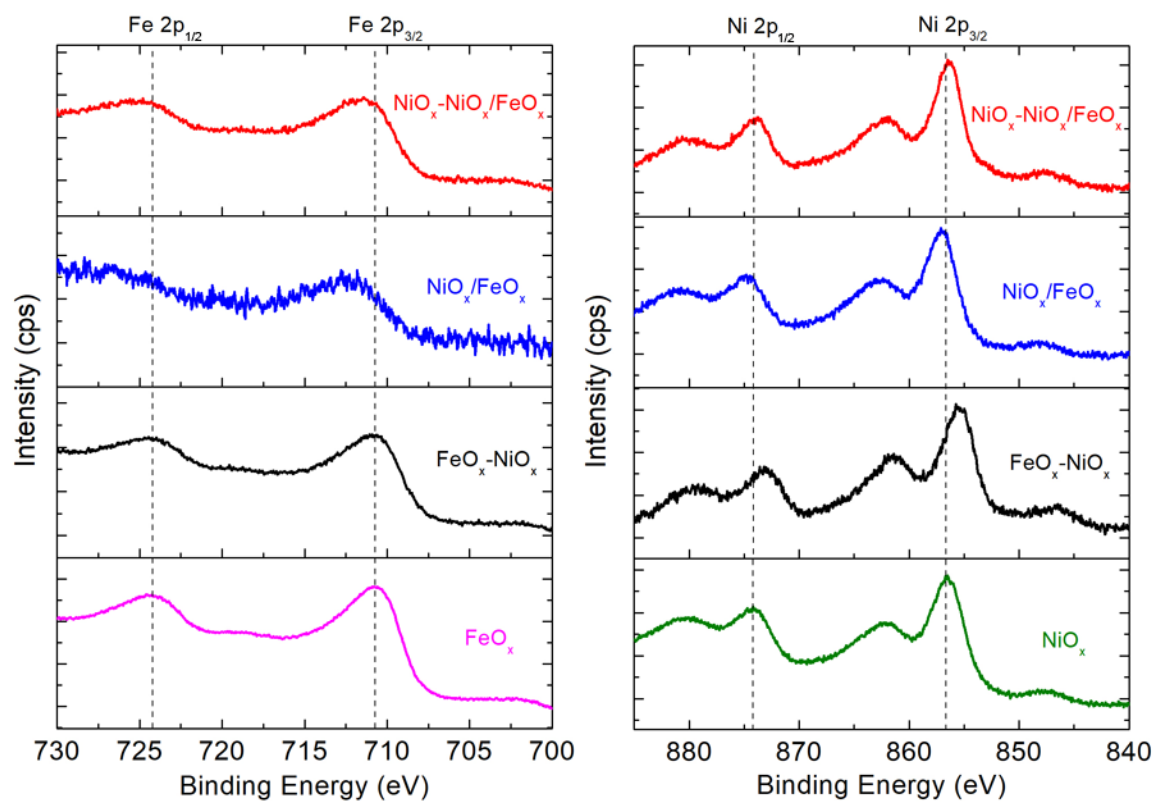


Figure S2. XPS spectra of Fe 2p and Ni 2p electrons for nanoparticles with different morphologies: NiO_x-NiO_x/FeO_x core-mixed shell (red), NiO_x/FeO_x alloy (blue), FeO_x-NiO_x core-shell (black), FeO_x (pink), and NiO_x (green).

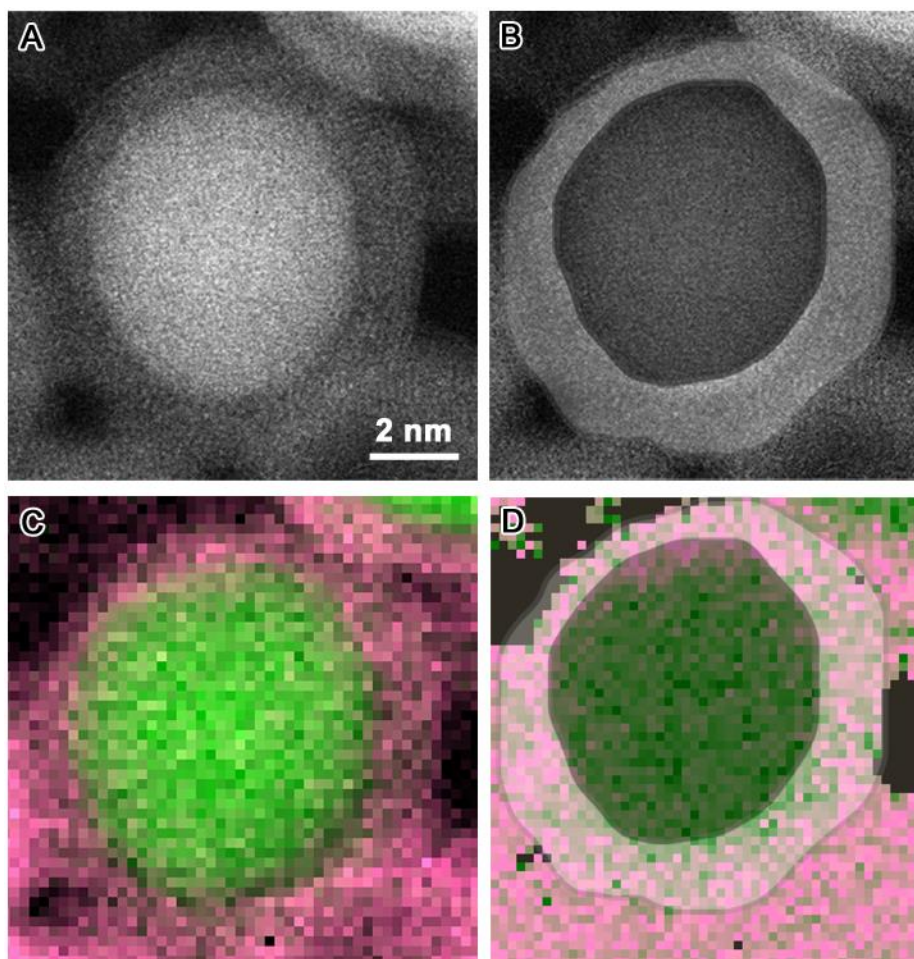


Figure S3. STEM images (A, B) and EELS maps (C, D) of the $\text{NiO}_x\text{-NiO}_x/\text{FeO}_x$ core-mixed shell structure on side-by-side panel displays. The highlighted areas in (C) and (D) illustrate the $\text{NiO}_x/\text{FeO}_x$ mixed shell for elemental quantitative analysis.

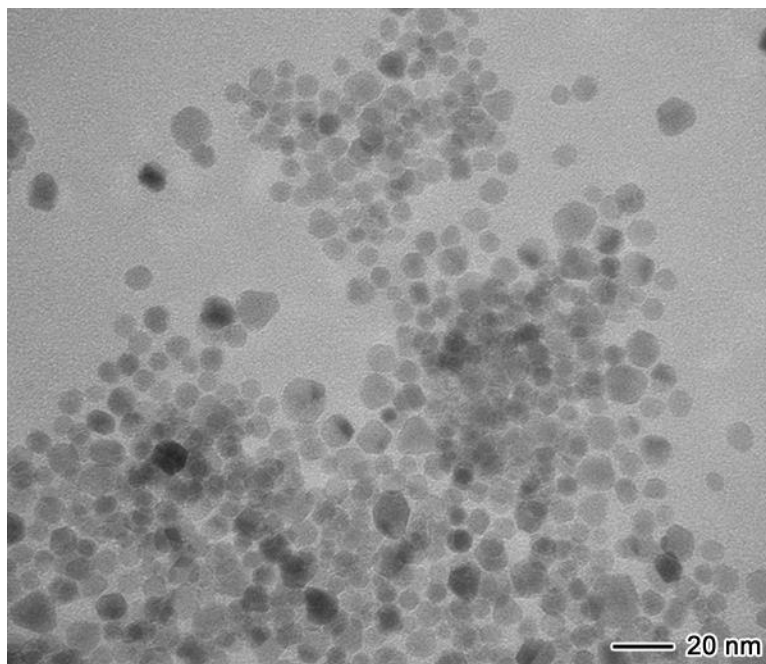


Figure S4. TEM image of FeO_x nanoparticles.

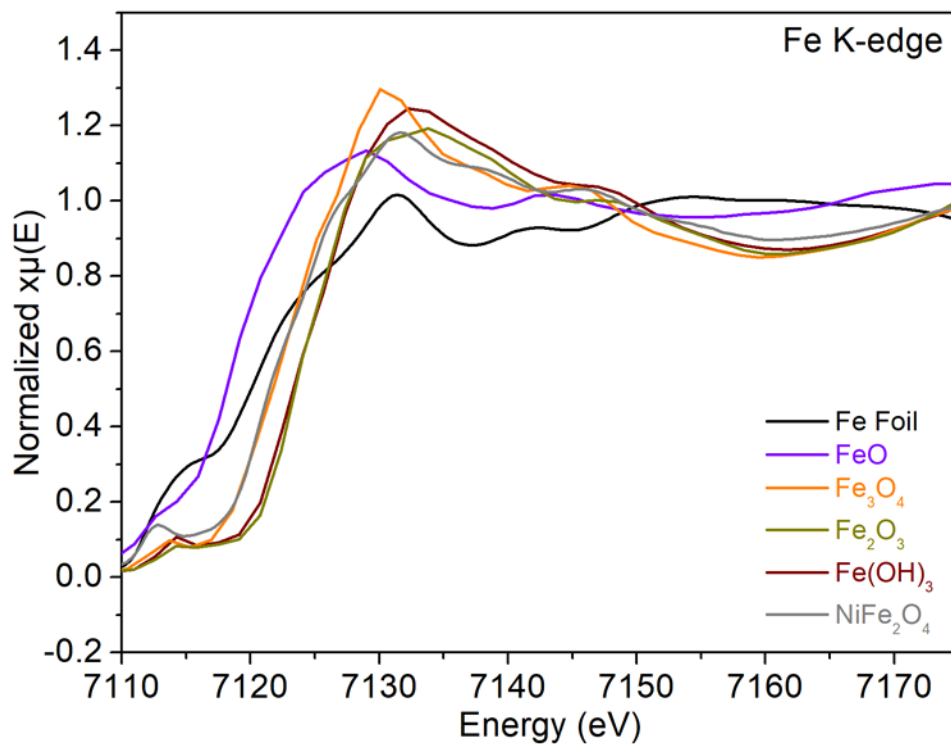


Figure S5. XAS spectra of Fe K-edge for Fe bulk standards: Fe foil (black), FeO (violet), Fe_3O_4 (orange), Fe_2O_3 (dark yellow), $\text{Fe}(\text{OH})_3$ (wine), and NiFe_2O_4 (grey).

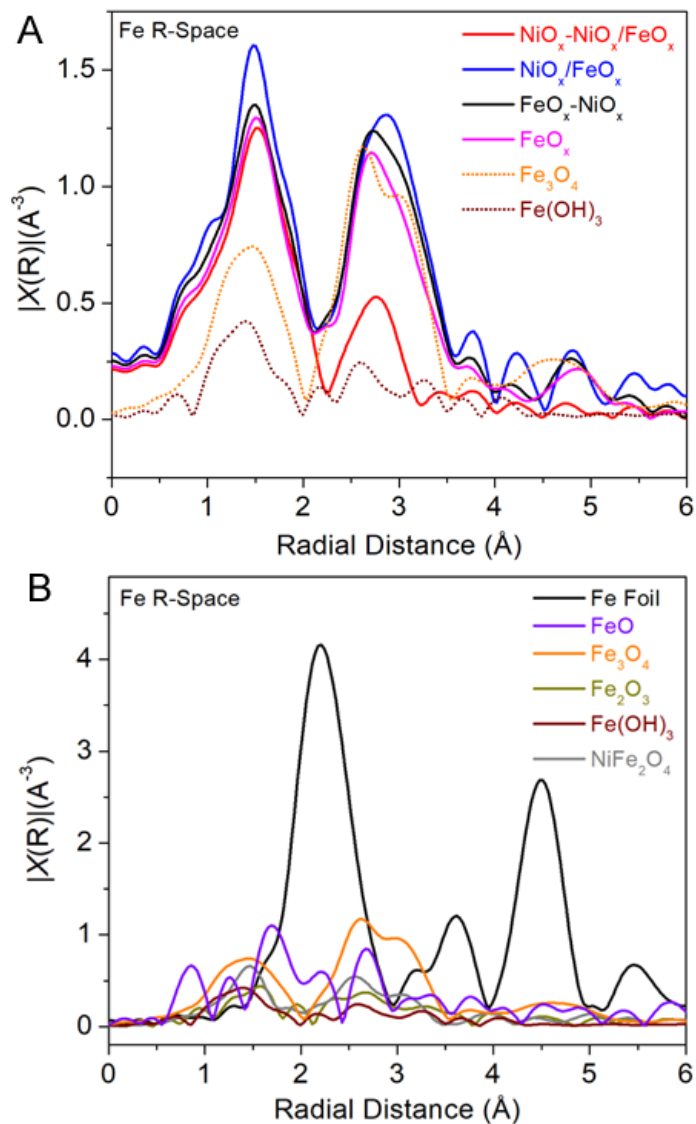


Figure S6. (A) EXAFS region of Fe K-edge for the nanoparticle catalysts: NiO_x-NiO_x/FeO_x core-mixed shell (red), NiO_x/FeO_x alloy (blue), FeO_x-NiO_x core-shell (black), and FeO_x (pink). The EXAFS region of selected Fe bulk standards were plotted in dash curves: Fe_3O_4 (orange) and $Fe(OH)_3$ (wine). (B) EXAFS region of Fe K-edge for Fe bulk standards: Fe foil (black), Fe_3O_4 (orange), Fe_2O_3 (dark yellow), $Fe(OH)_3$ (wine), and $NiFe_2O_4$ (grey). The plots were not corrected for the phase shift.

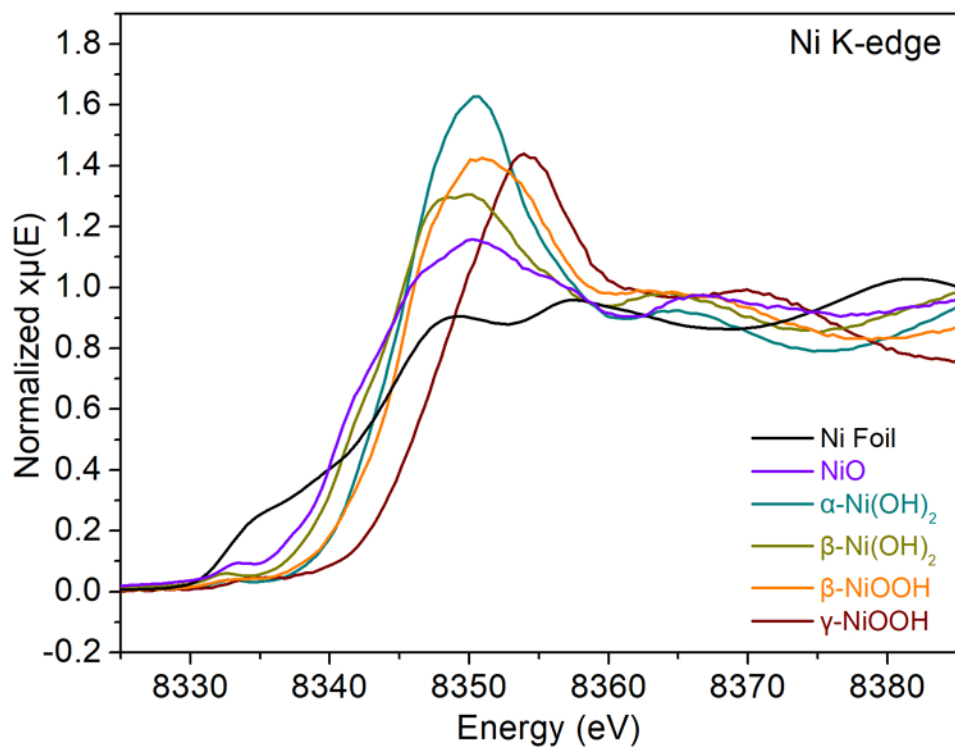


Figure S7. XAS spectra of Ni K-edge for Ni bulk standards: Ni foil (black), NiO (violet), α -Ni(OH)₂ (dark green), β -Ni(OH)₂ (dark yellow), β -NiOOH (orange), and γ -NiOOH (wine).

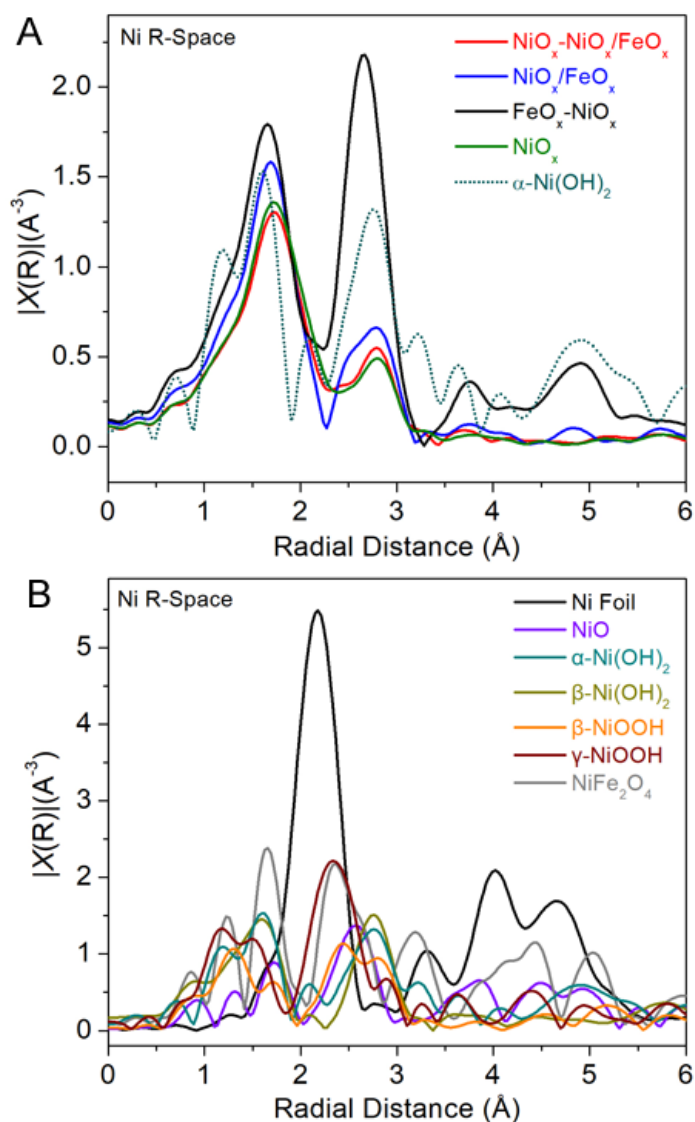


Figure S8. (A) EXAFS region of Ni K-edge for the nanoparticle catalysts: NiO_x-NiO_x/FeO_x core-mixed shell (red), NiO_x/FeO_x alloy (blue), FeO_x-NiO_x core-shell (black), and NiO_x (green). The EXAFS region of $\alpha-Ni(OH)_2$ bulk standard was plotted in a dark green dash curve. (B) EXAFS region of Ni K-edge for Ni bulk standards: Ni foil (black), NiO (violet), $\alpha-Ni(OH)_2$ (dark green), $\beta-Ni(OH)_2$ (dark yellow), $\beta-NiOOH$ (orange), $\gamma-NiOOH$ (wine), and $NiFe_2O_4$ (grey). The plots were not corrected for the phase shift.

Table S2. TOF values for each nanocatalyst calculated based on the Ni concentration either from the ICP-MS analysis ($\text{TOF}_{\text{ICP-MS}}$) or the redox wave integration ($\text{TOF}_{\text{redox wave}}$) assuming 1 or 1.5 electron transfer per Ni atom.

nanocatalysts	$\text{TOF}_{\text{ICP-MS}} \text{ (s}^{-1}\text{)}$	$\text{TOF}_{\text{redox wave}} \text{ (s}^{-1}\text{)}$ ($m = 1$)	$\text{TOF}_{\text{redox wave}} \text{ (s}^{-1}\text{)}$ ($m = 1.5$)
$\text{NiO}_x\text{-NiO}_x/\text{FeO}_x$	1.175	5.46	8.19
$\text{NiO}_x/\text{FeO}_x$	0.090	2.13	3.20
$\text{FeO}_x\text{-NiO}_x$	0.003	0.15	0.22
NiO_x	0.006	0.10	0.16

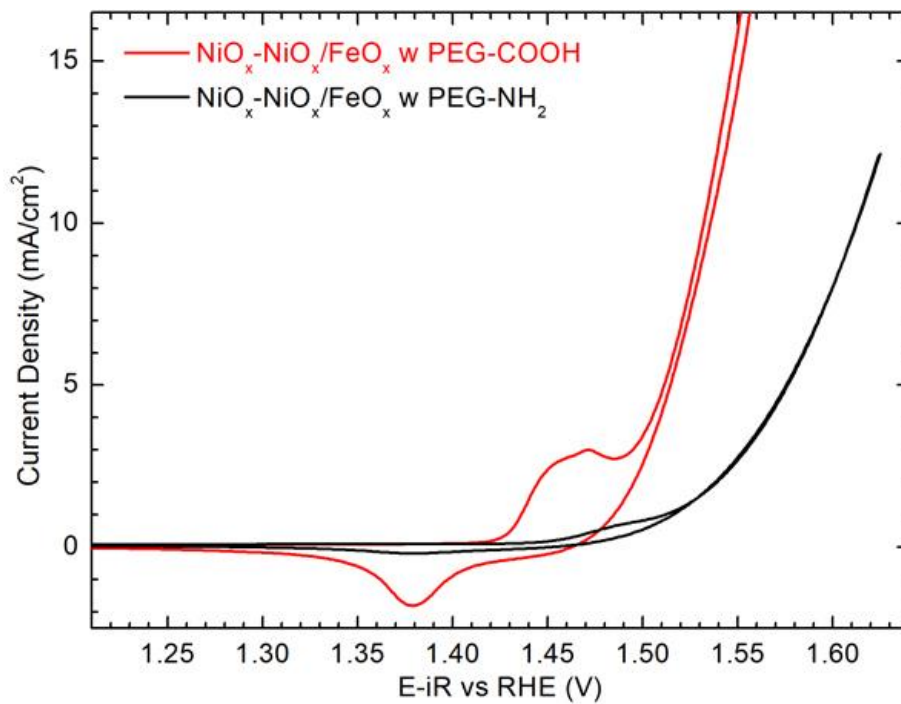


Figure S9. CV profiles of the nanoparticle catalysts obtained in 1 M KOH at a scan rate of 10 mV/s: NiO_x-NiO_x/FeO_x core-mixed shell with PEG-COOH surface ligand (red) and NiO_x-NiO_x/FeO_x core-mixed shell with PEG-NH₂ surface ligand (black).

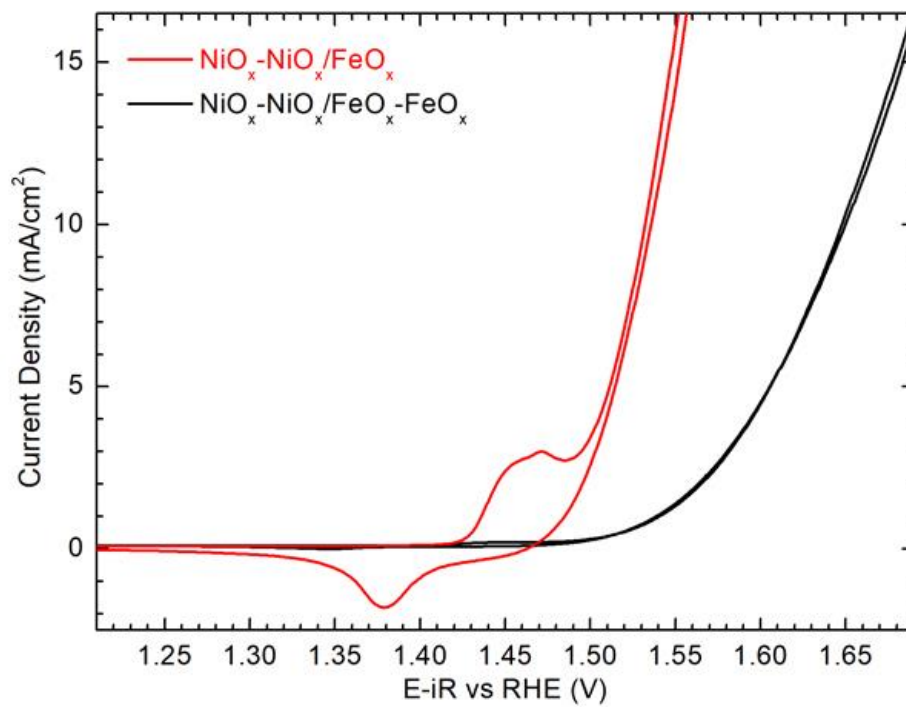


Figure S10. CV profiles of the nanoparticle catalysts obtained in 1 M KOH at a scan rate of 10 mV/s: NiO_x-NiO_x/FeO_x core-mixed shell (red) and NiO_x-NiO_x/FeO_x-FeO_x core-mixed shell-shell (black).

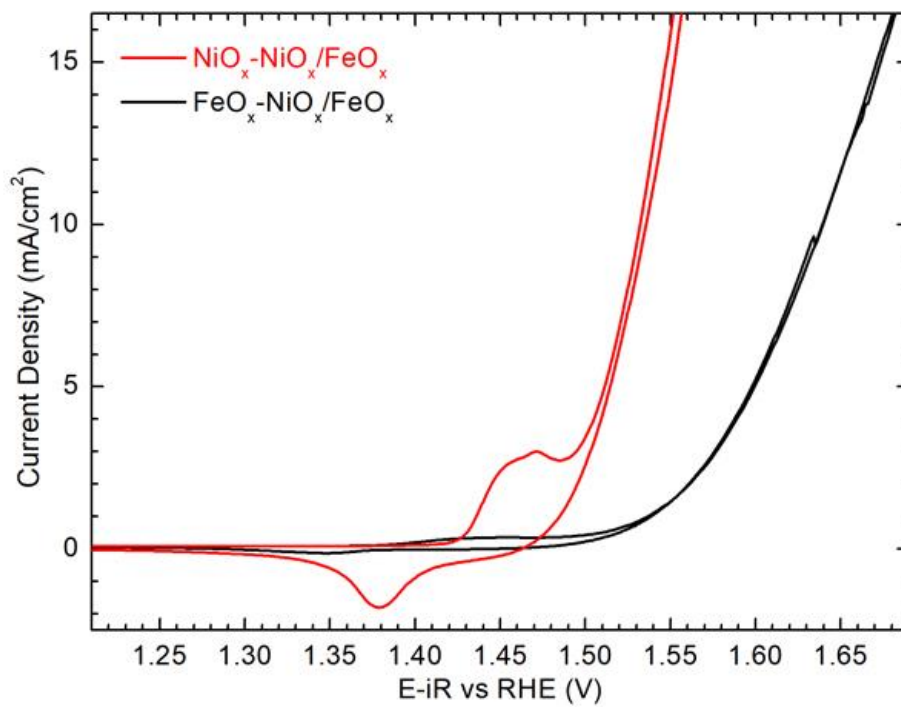


Figure S11. CV profiles of the nanoparticle catalysts obtained in 1 M KOH at a scan rate of 10 mV/s: NiO_x-NiO_x/FeO_x core-mixed shell (red) and FeO_x-NiO_x/FeO_x core-mixed shell (black).

References:

- (1) Egerton, R. F. *Electron Energy-Loss Spectroscopy in the Electron Microscope*, 3rd ed.; Springer Science+Business Media: New York, 2011; pp 270-277.
- (2) Stevens, M. B.; Enman, L. J.; Batchellor, A. S.; Cosby, M. R.; Vise, A. E.; Trang, C. D.; Boettcher, S. W., Measurement techniques for the study of thin film heterogeneous water oxidation electrocatalysts. *Chem. Mater.* **2016**, 29 (1), 120-140.
- (3) Smith, R. D. L.; Berlinguette, C. P., Accounting for the dynamic oxidative behavior of nickel anodes. *J. Am. Chem. Soc.* **2016**, 138 (5), 1561-1567.